SAND2011-2895C

Z-Backlighter facility upgrades: A path to short/long pulse, multi-frame, multi-color x-ray backlighting at the Z-Accelerator

Jens Schwarz[a], Patrick Rambo[a], Matthias Geissel[a], Mark Kimmel[a], Marius Schollmeier[a], Ian Smith[a], John Bellum[b], Damon Kletecka[c], Adam Sefkow[a], Douglas Smith[d], and Briggs Atherton[a]

[a]Sandia National Laboratories, Albuquerque, NM 87185
[b]Sandia Staffing Alliance, LLC, Albuquerque, NM 87110
[c]LMATA Government Services, LLC., Albuquerque, NM 87109
[d]Plymouth Grating Laboratory, Carver, MA 02330

ABSTRACT

We discuss upgrades and development currently underway at the Z-Backlighter facility. Among them are a new optical parametric chirped pulse amplifier (OPCPA) front end, 94 cm × 42 cm multi layer dielectric (MLD) gratings, dichroic laser beam transport studies, 25 keV x-ray source development, and a major target area expansion. These upgrades will pave the way for short/long pulse, multi-frame, multi-color x-ray backlighting at the Z-Accelerator.

Keywords: Petawatt Laser, OPCPA, MLD gratings, laser damage

1. INTRODUCTION

Since 2001 the Z-Backlighter facility at Sandia National Laboratories (see Fig. 1) has been operating the Z-Beamlet laser[1] (ns, kJ class at 527 nm) in order to radiograph high energy density physics (HEDP) events at the center of the Z-Accelerator.[2] In recent years our facility has added a short pulse laser capability. Two options of operation exist. The 100 TW option (100 J, 500 fs, 1054 nm) takes the 15 cm diameter sub-aperture beam at the output of the main amplifier and temporally compresses the beam in building 986 where it is propagated to a dedicated target area (100 TW target area). The second option takes that same 15 cm diameter beam and beam expands it as it propagates over to building 983 where it is temporally compressed. This laser chain is called Z-Petawatt (ZPW)[3] and operates at 500 J, 500 fs, and 1054 nm. This system can create x-ray backlighting energies > 25 keV which will allow us to probe deeper into the HEDP event. In addition the reduced pulsewidth will significantly improve motion blurring. We report here on several upgrades to our laser and facility that are currently pursued.

2. OPCPA UPGRADE

Our current OPCPA[3] front end operates at 1054 nm, 50 mJ, and 10 Hz with a stretched pulsewidth of 2 ns and a chirp of 4 nm/ns (1.1×10^{-3} THz/ps). This seed beam is amplified in two double passed 16 mm diameter and 25 mm diameter Phosphate:Glass amplifiers to yield the required 5 J input energy into the main cavity amplifiers. Since the commisioning about 8 years ago, the Z-Backlighter facility has expanded considerably and we now have a demand for much higher OPCPA output energies. Higher broadband OPCPA output can be used to lower subsequent amplifier gains, thus reducing gain narrowing and increasing bandwidth. A short pulse damage testing station was built[4] a few years ago and would benefit from higher energies by allowing larger area damage testing. Advanced experiments at the 100 TW target area require short pulse probe beams as well as short pulse optical triggers for streak cameras, both of which require more energy than is currently available.

Further author information: jschwar@sandia.gov

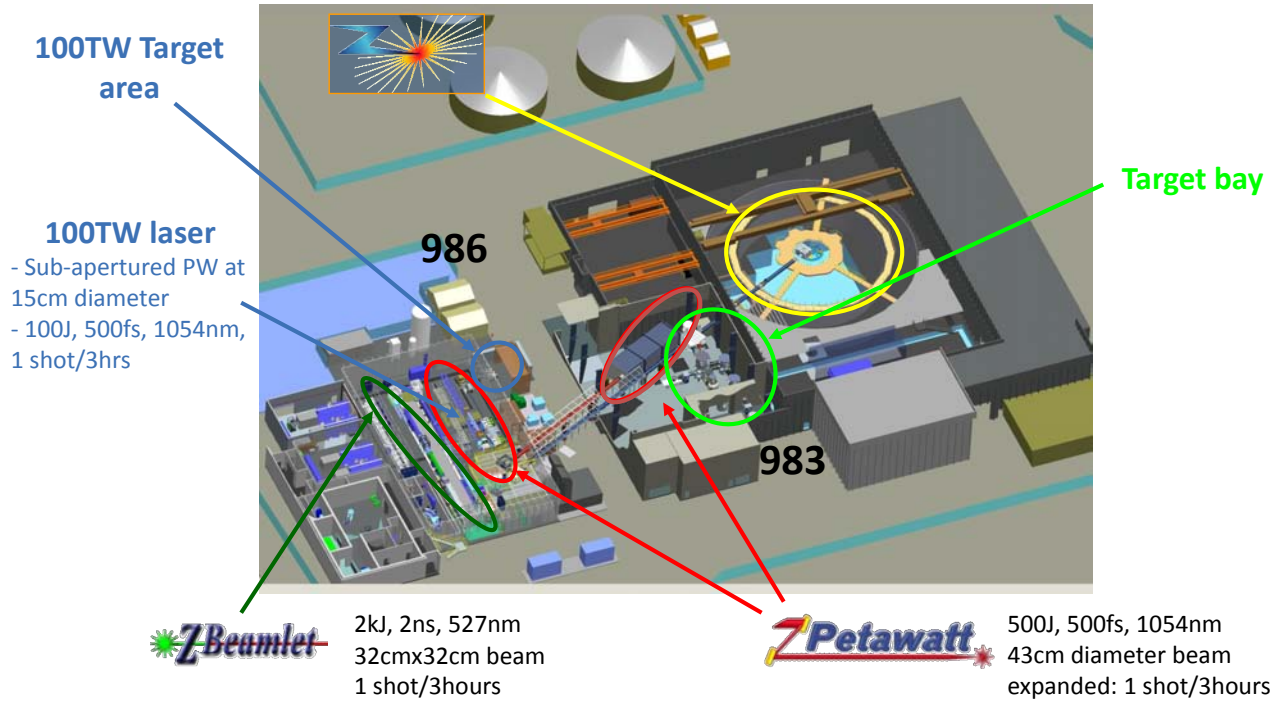

Figure 1. Overview of the Z-Backlighter laser facility. The Z-Beamlet laser and the Z-Petatwatt laser are located at the south side of building 986. The 100 TW laser is a subapertured part of the Z-Petawatt laser and its temporal compressor vessel, beam line, and target area are located at the north side of building 986. The PW beam option is beam expanded as it propagates through the bridge towards building 983 (Target bay) where its temporal compressor chamber is housed.

Table 1. OPCPA system parameters as well as the calculated energy and spectral bandwidth at each OPA stage.

	Signal energy (mJ)	Pump energy intensity (mJ:MW/cm^2)	Output energy (mJ)	Crystal & length (mm)	$\Delta\lambda$, $\Delta\tau$ (nm:ns)	signal beam ϕ FWHM (mm)	Gain
OPA 1	250×10^{-9}	70:520	0.050	LBO 2 ea. 25	8.7:2.2	2	10^5
OPA 2	0.05	120:800	30	LBO 2 ea. 13	14:3.5	1.5	600
OPA 3	30	400:750	170	BBO 6	15.3:3.85	3.7	6
OPA 4	150	4000:400	1500	BBO 9	15.7:4	16	10

The new OPCPA system is designed to yield >1 J of stretched 1054 nm signal energy at a repetition rate of 2 Hz with a spectral bandwidth of >12 nm. This energy output is sufficient to satisfy the facility needs and is enough to seed a double passed 25 mm rod amplifier directly (without going through the 16 mm amp first). The following design is based on a pump source that yields 5.5 J, 532 nm, at 2 Hz with a pulsewidth of 4.3 ns.[5] Simuilations were performed using a modified SNLO code from Arlee Smith.[6] This code included the ability to model supergaussian pump, signal, and idler beams both in space and time. Table 1 shows the OPCPA system parameters as well as the calculated energy and spectral bandwidth at each OPA stage. Figure 2 shows the simulated gain and output energies for all 4 OPA stages. All OPA stages (except for OPA 1) operate in the saturated regime. The pump power levels have been kept below 4 J/cm^2 of fluence at any OPA stage. Beamsize, spectral bandwidth, and temporal pulsewidth have been modeled as well and are shown in Table 1. The simulation suggests that the desired output energy of > 1 J should be achievable. At 16 nm of spectral bandwidth, this output could support pulses as short as 100 fs after temporal compression which means that this system could serve as a stand alone 10 TW system at 2 Hz repetition rate. Figure 3 shows the new OPCPA system at its current stage of development. The pump laser (right side) is operational and the basic beam transport infrastructure for the OPA pump and signal beam is in place.

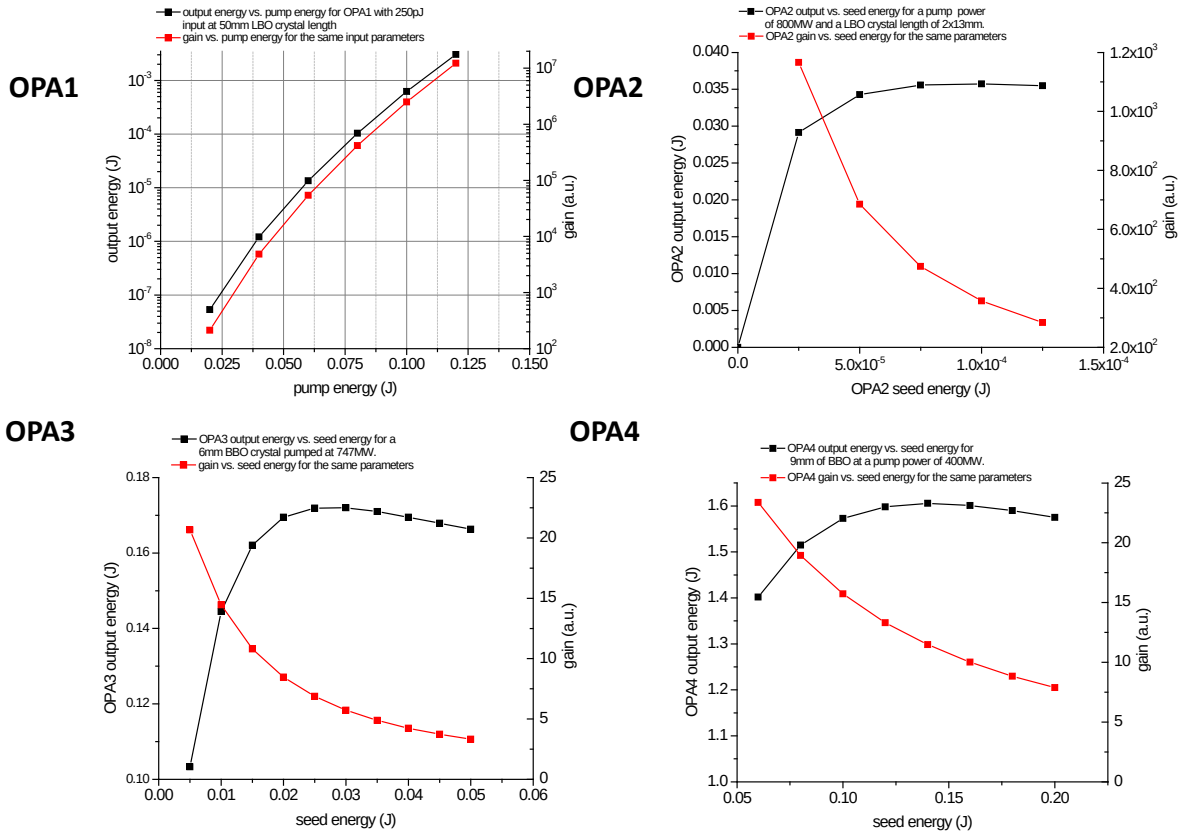

Figure 2. Simulated gain and output energies for all 4 OPA stages.

Figure 3. (left) Spatial filter/transport telescopes in place for signal and pump beam of all 4 OPA stages; (right) 5.5 J, 532 nm, 2 Hz pump laser source.

3. MULTILAYER DIELECTRIC (MLD) GRATINGS

Sandia's Petawatt laser beam diameter is currently around 43 cm which corresponds to an area of 1450 cm^2. The damage threshold for our LLNL Nova gold gratings is estimated at 400 mJ/cm^2.[7,8] With a safety margin to account for 1:1.3 beam modulation, fluences are limited to 300 mJ/cm^2 corresponding to 450 J output energy which can be expected at peak compression (< 1 ps). However, the Z-Petawatt main beam amplifiers can theoretically produce up to 5 kJ of 1054 nm laser light in a 32 cm × 32 cm beam.[1] In order to more efficiently use this energy, it has been decided to replace the old gold gratings with higher damage threshold MLD gratings. This has been done in two stages. First, we replaced the 42 cm × 21 cm gold gratings (1480 l/mm) in our 100 TW laser chain with 60 cm × 21 cm MLD gratings (1740 l/mm) from Plymouth Grating Laboratory (PGL).[9] At that point, the 1480 l/mm grating stretcher was replaced by a new 1740 l/mm MLD stretcher in order to compensate the higher order dispersion terms. It was demonstrated that since the grating change two years ago, our 100 TW beam line has in fact operated at > 200 TW with no visible damage on any of the gratings. This performance gave confidence for a second phase of MLD upgrades at which point Sandia acquired 4 ea. of 94 cm × 42 cm MLD gratings at 1740 l/mm.

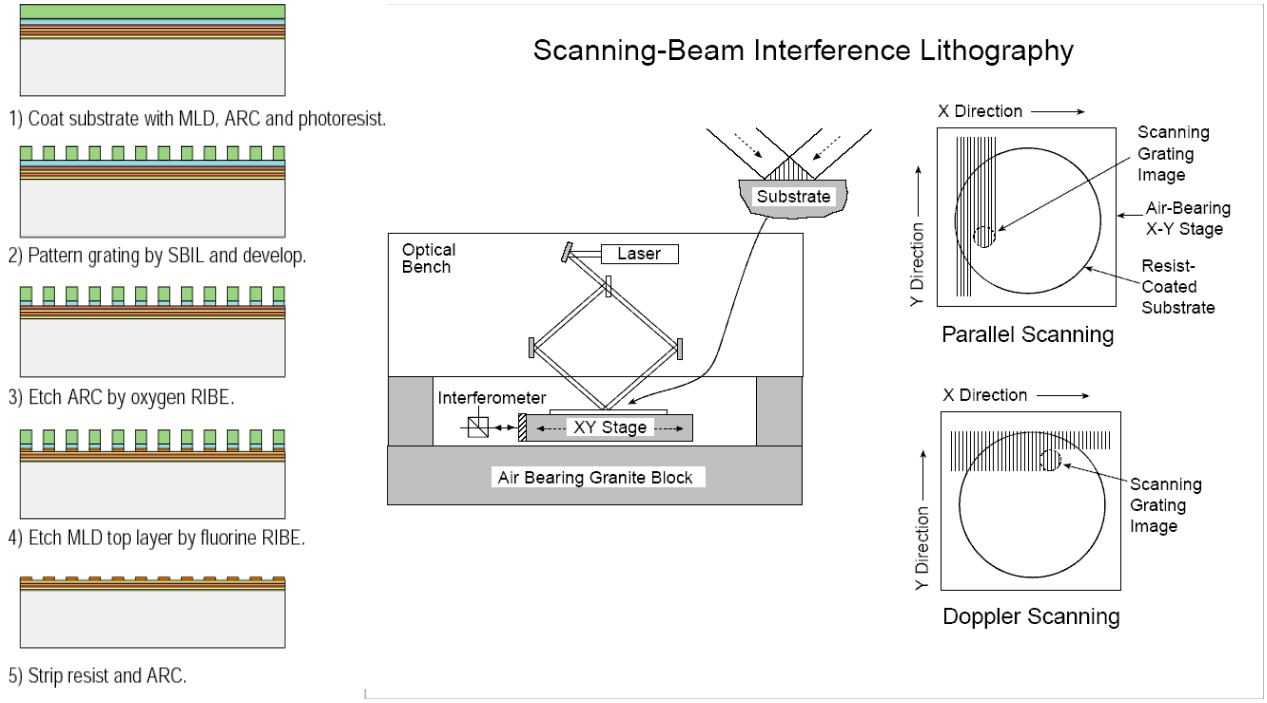

Figure 4. (left) The MLD grating Process, (right) A simplified view of scanning beam interference lithography. The key is the stage interferometer which allows fringe locking to the substrate. Scanning can then be performed in a parallel or perpendicular direction of the fringes as shown.

The MLD Grating[10] process is shown schematically in Fig. 4. A thin film dielectric stack reflector is coated onto a fused silica substrate. The coating is made by electron-beam evaporation of 26 layers hafnium oxide and silicon dioxide to form the reflector with a thick silica layer on top to form the grating. The coating is made with additional Oxygen ion bombardment to control bending due to stress when the grating is used in the final vacuum environment. After MLD coating, an absorbing layer (ARC) is applied to suppress electric field standing waves, followed by a layer of photoresist (Fig. 4, step 1). The photoresist is exposed using interference lithography and developed to form grating lines (step2). The grating has sufficient diffraction efficiency at this point to verify the diffracted wavefront quality with a large aperture interferometer. The grating is then placed in a large vacuum chamber to transfer the grating pattern into the top silica layer using a reactive ion etch process. In this chamber first the ARC layer is removed (step 3) and then the silica layer is etched with the

grating pattern (step 4). The remaining ARC and Photoresist are removed in a final aggressive cleaning process (step 5). This last step is critical to achieving a high laser damage threshold but also must be performed without inflicting damage to the delicate grating and MLD coating.

The gratings are exposed using a unique scanning-beam interference lithography (SBIL) process.[11] This process, developed at the Massachusetts Institute of Technology, generates an interference fringe pattern with small beams and then scans this small beam in an overlapping pattern over the large area of the gratings (Fig. 4 (right)). The fringes in the small beam are spatially locked to the substrate using interferometry to accurately locate substrate position at all times. The size limit for the written grating will now only depend on the travel limits of the x-y stage moving the substrate (in this case 960 mm × 550 mm). In addition to writing large sizes this technique has several advantages including: 1) improved dose control for exposure, 2) excellent uniformity of grating duty cycle, 3) very accurate period control, 4) automatic change of fringe frequency from 50 to 5000 lines/mm, 5) a potential to adjust period in real time while writing. Grating writing on this instrument is fully automated with exposures for full size gratings taking from 18 to 30 hours. The instrument is housed in a temperature-controlled enclosure to reduce the effects of optical errors from atmospheric turbulence.

Figure 5 (a) shows the 1st order diffraction efficiency across the whole grating surface for one of the 94 cm × 42 cm MLD gratings. One can see that the average efficiency is above 96% which leads to an overall grating compressor throughput of $> 85\,\%$. Figure 5 (b) depicts the diffracted wavefront in 1st order. The peak to valley (PV) wavefront deformation is $< 1/5$ wave and the root mean square (RMS) is 1/30 wave at 1054 nm.

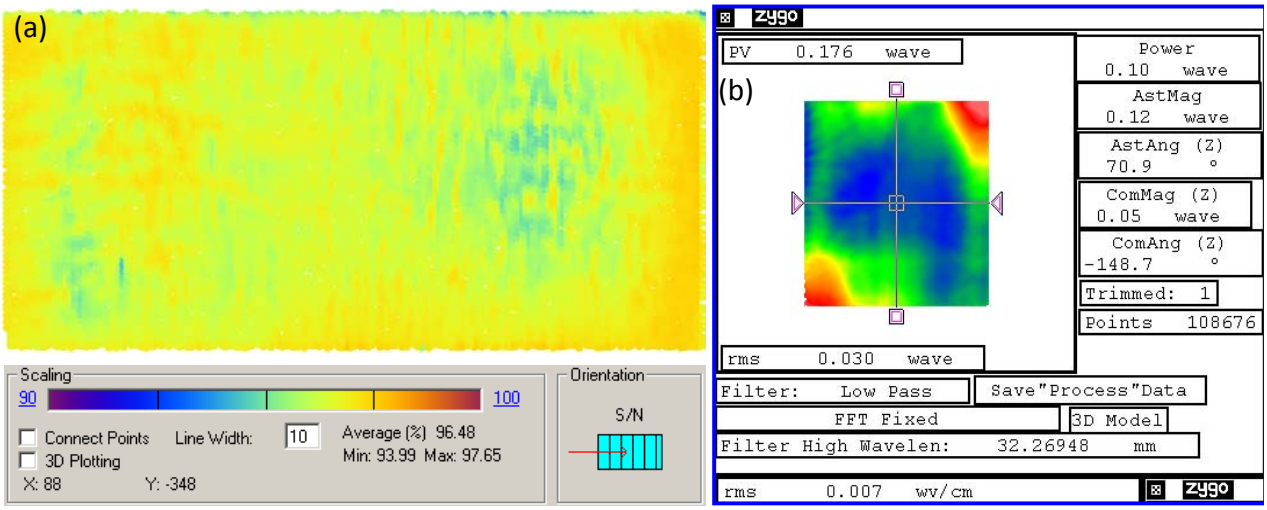

Figure 5. (a) Diffraction efficiency in 1st order, (b) Diffracted wavefront in 1st order.

Figure 6 (a) shows an SEM image of a witness grating. Figure 6 (b) depicts the President of Plymouth Grating Laboratories, Doug Smith, as he illuminates one of the gratings with an Hg lamp at Littrow angle. Laser damage thresholds have been specified at 1.0 J/cm^2 at 500 fs and 3.2 J/cm^2 at 10 ps in the right hand cross-section of the beam for a 72° angle of incidence. Table 2 shows the expected laser output energies for various configurations. A safe operation de-rating of 1:1.3 has been applied to account for intensity fluctuations across the laser beam profile. Looking at table 2 one can see that > 1 PW operation can be achieved, even at a high contrast configuration. Long pulse operation yields up to 2.2 kJ of energy which is needed for x-ray backlighting on the Z-Accelerator.

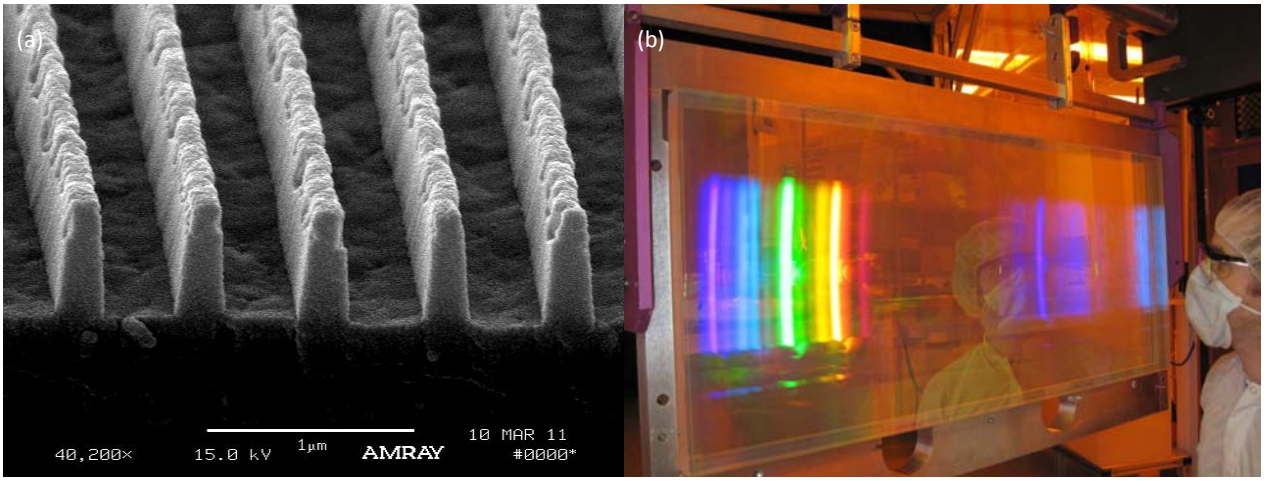

Figure 6. (a) SEM image of a witness grating (b) Diffracted light at Litrow angle using an Hg lamp

Table 2. Various grating compressor configurations and their associated performance parameters. Note that the spectral bandwidth is for a fully cleared spectrum spatially across the beam. The center part of the beam in each case contains a larger spectrum.

Configuration	spectral bandwidth (nm)	beam footprint	Maximum/Safe energy at 500 fs (J)	Maximum/Safe energy at 10 ps (J)
Normal Operation	8	32 cm × 24 cm = 768 cm^2	768/590	2460/1890
High Contrast	12	32 cm × 22 cm = 704 cm^2	704/542	2253/1733
Long Pulse Operation	< 1 10 ps	32 cm × 27 cm = 864 cm^2	NA	2765/2127

4. DICHROIC BEAM TRANSPORT

In order to achieve multi-frame, short/long pulse backlighting on the Z-Accelerator one must be able to co-propagate the 1054 nm short pulse and the 527 nm long pulse beam into the center section of the Z-Machine. The required damage threshold for these 75 cm diameter optics are > 1 J/cm^2 for the short pulse (to match the damage fluence of the grating) and > 10 J/cm^2 for the long pulse laser. Further challenges arise from the fact that the final focusing optics on top of the Z-Machine allow for flexible pointing into the center section such that the coatings have to cover the following parameter space: reflectivity in S and P polarization > 99.6% at angles of incidence (AOI) from 24° to 46° at 527 nm ± 3 nm and at the same time for 1054 nm ± 6 nm. This coating challenge was met in 2009 with a 50 layer hafnia-silica ion assisted deposition coating run on the 75 cm diameter fold mirror in the final optics assembly (FOA).[12]

Figure 7 shows a spectral photometer trace (red) of this optic at AOI of 25° (a) and 45° (b) compared to the coating design (black line). Laser induced damage threshold (LIDT) for the long pulse 527 nm beam was measured at SPICA[13] according to NIF-MEL LIDT specifications. The reported LIDTs were 16 J/cm^2 at AOI of 25° and 19 J/cm^2 at AOI of 45°, both measured in the right hand cross-section of the beam. Short pulse vacuum damage testing was performed at our Z-Backlighter facility using a 400 fs beam at 1054 nm.[4] At AOI of 35° a damage threshold of 1.38 J/cm^2 was reported in the right hand cross-section. One can see that all coating challenges could be met for the final focusing optics. The last remaining complex coating will be the harmonic beam combiner having a high transmission at 527 nm and a high reflectivity at 1054 nm, 45° S-polarization.

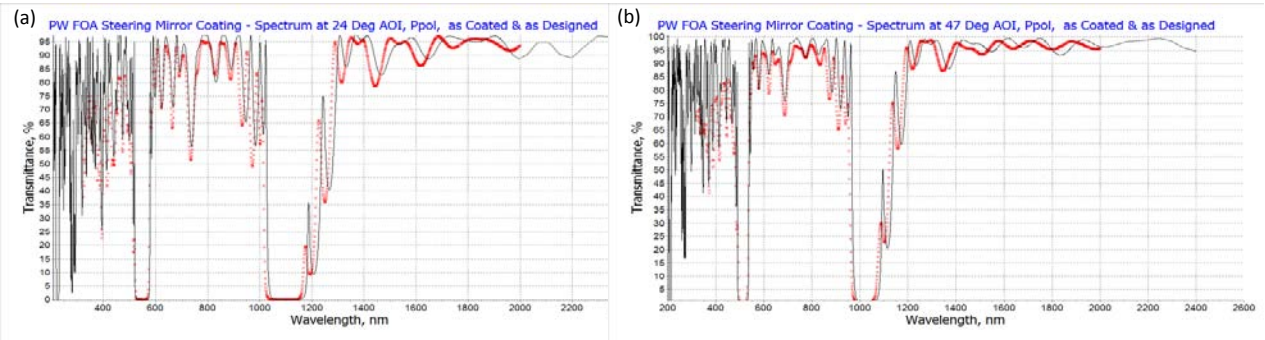

Figure 7. (a) Comparison of spectral photometer trace (red) and the coating design (black) for 25° AOI and (b) 45° AOI.

5. ZPW X-RAY SOURCE DEVELOPMENT

Using Z-Beamlet, point-projection X-ray backlighting on the Z-Accelerator has been performed since 2001.[14] In 2003 a bent-crystal imaging system was installed[15,16] which ultimately improved image resolution down to 20μm. A multi-frame backlighting capability was installed on Z-Beamlet in 2006[17] which now allows one to take time delayed images either at the normal 6.15 keV x-ray level or a combination of 6.15 keV for one time delay and 1.87 keV at some other time delay.[18] This shows that two x-ray color multi-frame x-ray backlighting has already been demonstrated on Z-Beamlet alone. We would like to add the 25 keV x-ray capability of ZPW (possibly with its own multi-frame backlighting capability) to probe further into the plasmas and to improve motion blur. At

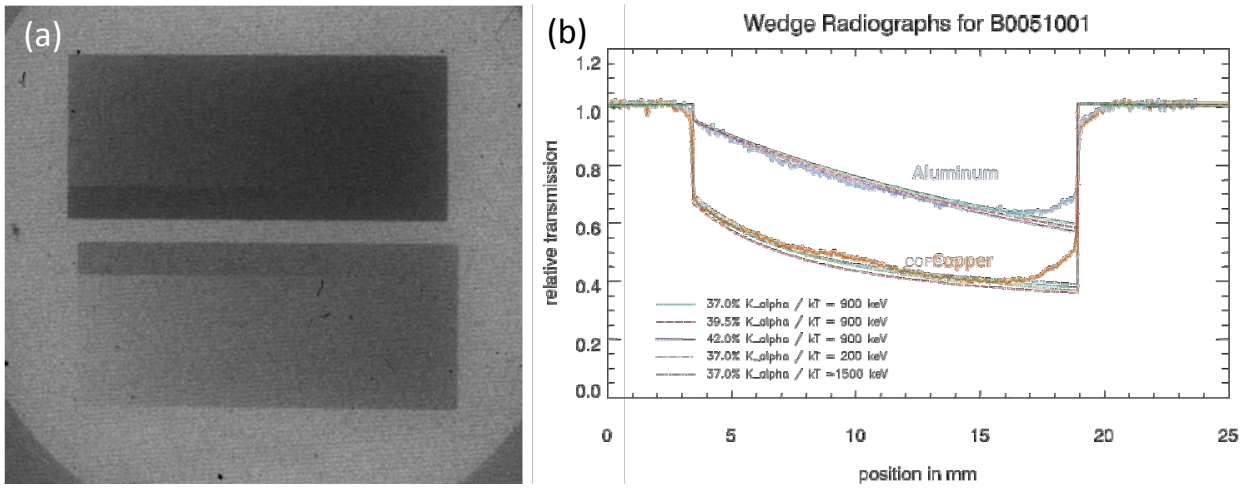

Figure 8. (a) Contact image radiographs from copper and aluminum wedges, (b) Lineout was analyzed by fitting the K_α and bremsstrahlung spectra to the function cited in the text below.

this point, no suitable crystal has been identified to perform bent-crystal imaging at 25 keV. Therefore we focus on point projection, meaning the characterization of the x-ray source as well as the x-ray imaging properties.

5.1 X-ray Spectrum and Conversion Efficiency

A combination of Sn flat foils, mass reduced Sn foils (250 μm sides and $< 100\mu$m thickness), and cubic Sn targets with 100 μm sides over a range of intensities from 10^{18} W/cm^2 to 10^{20} W/cm^2 were characterized. The source spectrum was obtained through three different approaches. The first was using wedges, one made from copper and the other from aluminum. The second approach was using a single photon counting CCD, while the third was using a highly ordered pyrolytic graphite (HOPG) crystal spectrometer.

The copper and aluminum wedges were placed in-contact with an image plate (see Fig. 8(a)). A lineout from the image was analyzed by fitting the K_α and bremsstrahlung spectra with the following distribution: $F(E_{ph}) = const./kT \times e^{-E_{ph}/kT}$, where k is the Boltzmann constant, T is the temperature of the radiation, and E_{ph} is the photon energy. The lineout and best fit are shown in Fig. 8(b).

The analysis showed that the spectrum consists of 39% K-shell radiation and 61% bremsstrahlung, giving an efficiency of $1 - 2 \times 10^{-4}$ from laser energy into the K_α-line. The fit assumed a window of 22-28 keV for K-shell radiation. The bremsstrahlung contribution could be best explained by a temperature parameter of $kT = 400 - 900$ keV. The influence of the ratio of K-shell radiation versus Bremsstrahlung was much more significant in the data-fit than the temperature of the continuum radiation, which lead to the high uncertainty in the value for kT.

The second spectral method was using a single photon counting deep depletion CCD and the third method an x-ray spectrometer with a 2 mm thick HOPG crystal. The results of these measurements are shown in Fig. 9. The blue curve in Fig. 9(a) shows the corrected spectrum from the single photon counting CCD. The HOPG spectrum is in good agreement with the single photon counting camera (see Fig. 9(b)), and it provides a measurement for the intensity ratio between K_α and K_β lines.

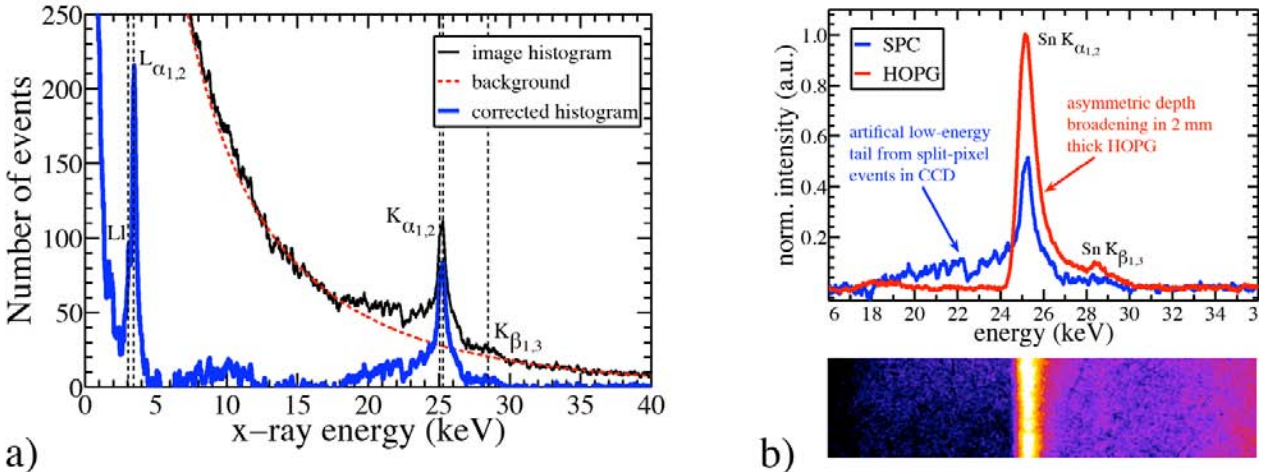

Figure 9. Comparison of 25 keV Spectrum from (a) Single Photon Counter measurements with a deep depletion CCD, an integrated conversion efficiency of $1 - 2 \times 10^{-4}$ from laser light into K-shell X-rays. (b) A 2 mm HOPG crystal spectrum proves good agreement and shows the small contribution of K_β radiation to the K-shell spectrum

The experimental K_α laser energy conversion efficiencies of these sources are 1 to 2 $\times 10^{-4}$ and are shown in Fig. 10(a). Flat foils had slightly higher efficiencies but lead to poor spatial resolution for point projection imaging. Cube targets with dimensions of 100 μm per side were the best compromise for the 100 TW Target Area, but experiments on the Z-Accelerator will have to start with larger targets until sufficiently precise pointing accuracy can be achieved for Z-Petawatt in the Z-Machine center section. These efficiencies measured at Sandia agree well with published data such as those of Park.[19] It has proven to be desirable to stay with lower intensities, such that the high energy bremsstrahlung component (noise) of the spectrum gets reduced, while the 25 keV signal remains high. This has motivated the use of 10 ps scale laser pulses on ZPW for backlighting. This in turn results in higher laser energies and greater x-ray flux for backlighting.

Fully electromagnetic, relativistic, explicit, and kinetic particle-in-cell simulations are employed to model laser-target interactions self-consistently at solid density by launching laser fields from the boundary. This approach is in contrast to models using implicit, hybrid fluid-kinetic, or ad-hoc electron energy distribution function injection methods, all of which inherently allow free numerical parameters. These simulations were used

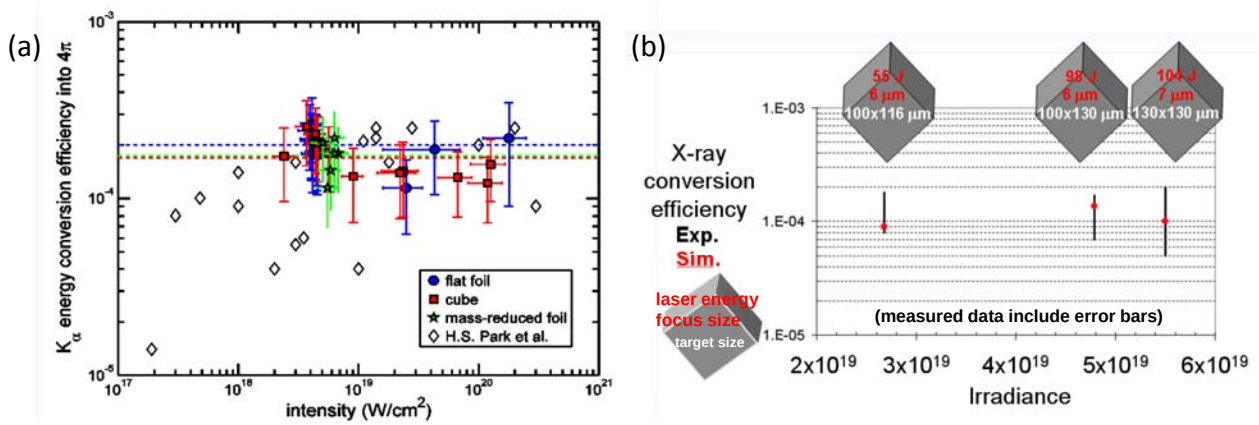

Figure 10. (a) The K_α efficiencies of Tin (Sn) from flat foils and cubes into 4π radians. Colored symbols with error bars were measured at Sandia. Open symbols were taken from.[19] (b) Comparison between the LSP simulation (red dots) and experiment with error bars (black lines).

to model K_α efficiencies versus irradiance. The comparison of K_α efficiencies between simulation and experiment is shown in Fig. 10(b). It is noteworthy that the LSP[20] simulations were carried out using measured laser and target parameters from experiments, and no free numerical parameters were allowed in the model.

5.2 Imaging Properties of the X-Ray Source

To use point projection, a number of conditions must be satisfied:

1. The x-ray source needs to be small enough to provide sufficient resolution,
2. The detector must be filtered such that both undesired X-ray background and z-pinch debris do not compromise the recorded image, and
3. The best compromise between field-of-view, spatial resolution and geometrical setup (i.e. distances between x-ray source, object and detector) needs to be determined.

The energetic electrons that are generated by ultra-intense lasers have lifetimes and kinetic energies which allow them to spread wide into the target. Therefore a large laser target leads to a deterioration of the spatial resolution with point-projection. Reduced mass targets and cubes were found to define the source size essentially by their geometric dimensions, e.g. 100 μm cube targets lead to a source size of about 100 μm. This dependency has been verified with various knife-edge measurements at Sandia. The following factors decide the geometry:

- For a given detector size, the field of view is larger the closer the detector is to the object.
- To protect the detector, it helps for the detector to be small and farther away from the object.
- The spatial resolution increases with the detector's proximity to the object.
- The available source position in the Z-Accelerator is 4 inch away from the object.

Considering all circumstances, a 2:1 magnification for the point-projection was chosen. Figure 11(b) shows a 2:1 magnified radiograph of a double liner test object (a) acquired in the 100 TW Target Chamber of Z-Petawatt with a 500 μm large Sn target. Both liners including their notch features are resolved well, but the limb darkening profile and edge sharpness suffer from a blur due to the large x-ray source size.

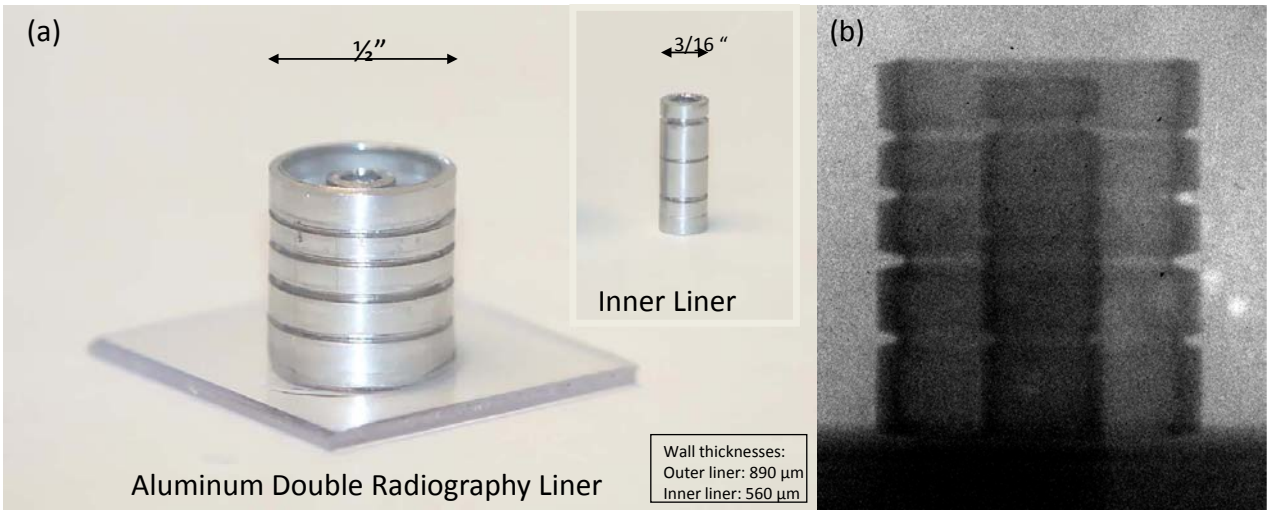

Figure 11. (a) Test object, a double aluminum liner. The outer liner diameter is 12.70 mm, the inner liner diameter is 4.763 mm. Grooves have been machined into the liners to verify imaging properties. (b) Radiography image of two nested aluminum liners.

The 2:1 radiograph test was achieved with a laser pulse width of 7 ps, a pulse energy of 100 J and a focus size of approximately 10 μm. A series of previous experiments showed that 50 μm of cadmium or 75 μm of indium are the best choice for a filter, allowing good transmission of 25 keV radiation while efficiently suppressing background between 0-20 keV as well as 30-60 keV. The slightly more favorable cadmium is used for 100 TW experiments while indium is used in the Z-Accelerator because of the expected destruction of the filter and the high toxicity of cadmium. The filter must be reinforced for debris protection, and the best combination of transmission and strength was found to be accomplished with 2 mm polyimide and 2 mm aluminum in sixteen 250 μm layers.

6. TARGET BAY

The Z-Backlighter facility currently has two target chambers dedicated for stand alone laser experiments. One is called the "calibration chamber" which is connected to Z-Beamlet and is mostly used for calibration and testing of experiments/technologies for Z-Machine experiments. The second target chamber is at the end of the 100 TW beamline and is used for a variety of experiments such as x-ray source development, particle acceleration, advanced backlighting experiments, and plasma mirror studies, all of which also tie in with Z-Accelerator experiments.

In order to increase the usability and experimental flexibility of our facility, it has been decided to install additional target chambers in our so called "Target Bay". Figure 12 shows how the new Target Bay is envisioned. Three more chambers have been added to compliment our current capability. They all have an octagonal shape with 1.5 m diameter and have the focusing optics placed outside the chamber in order to save space for the experimental apparatus inside the chamber.

- "Z Chamber" (upper right) for Beryllium and Z-Machine related experiments. This area is self-contained in order to prevent any possible Be contamination beyond the target area. This chamber can either receive Z-Beamlet or Z-Petawatt.
- "ZBL Chamber" (lower right) for dedicated Z-Beamlet experiments.
- "Z-Petawatt Chamber" (middle) for dedicated Z-Petawatt short pulse experiments. Previsions have been made to shoot Z-Beamlet into the same chamber at angles of 0°, 45°, 90°, and 180°.

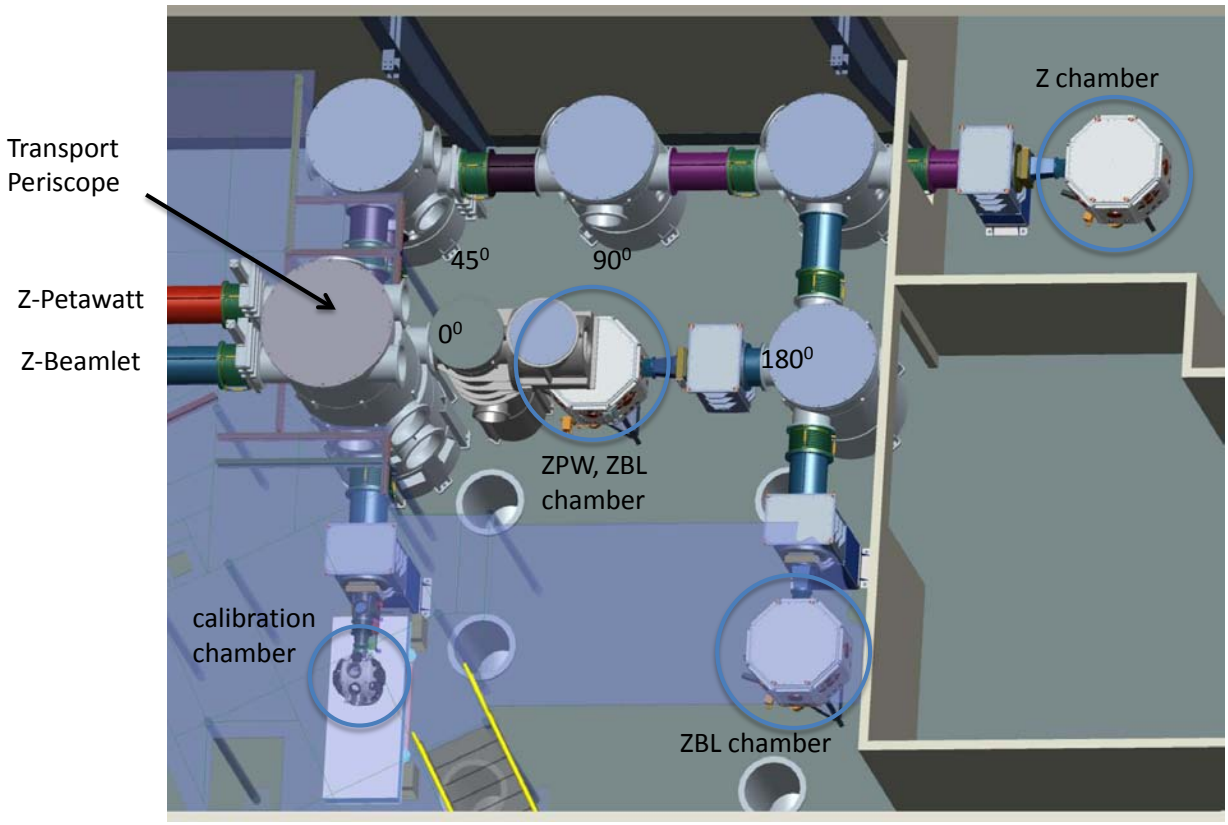

Figure 12. Layout of the target bay. One can see all four chambers, two of which can receive either ZPW or Z-Beamlet, the remaining two are dedicated to Z-Beamlet only. The beam transport tubes are color coded to help understand which part of the Target Bay can receive what type of laser beam. RED: Z-Petawatt only, BLUE: Z-Beamlet only, PURPLE: ZPW AND/OR Z-Beamlet.

Figure 13 shows the target bay as of March 2011. All vacuum vessels and target chambers have been received and have been placed. The remaining chambers still need additional vacuum infrastructure before they become operational. Furthermore, the target chambers need to be equipped with target manipulators (and similar infrastructure) to make them usable for experiments. Efforts are underway to continue the construction of this area.

7. CONCLUSION

- Multi-frame backlighting[17] has been shown to be a viable technique and could easily be implemented at ZPW.
- Two color backlighting has also been demonstrated[18] and will become an even more powerful tool with the addition of a 25 keV backlighting option.
- Sending a ZPW beam into the Z-Machine center section poses new challenges with respect to debris mitigation. This topic has not been discussed in this paper. However, a detailed description of our novel debris mitigation techniques for ZPW operation can be found elsewhere.[21]
- It has been demonstrated that we can fabricate complex dual wavelength optics with high damage thresholds for < 1 ps at 1054 nm and ns scale pulses at 527 nm[12] However, the fabrication of a dual wavelength combiner is still pending.

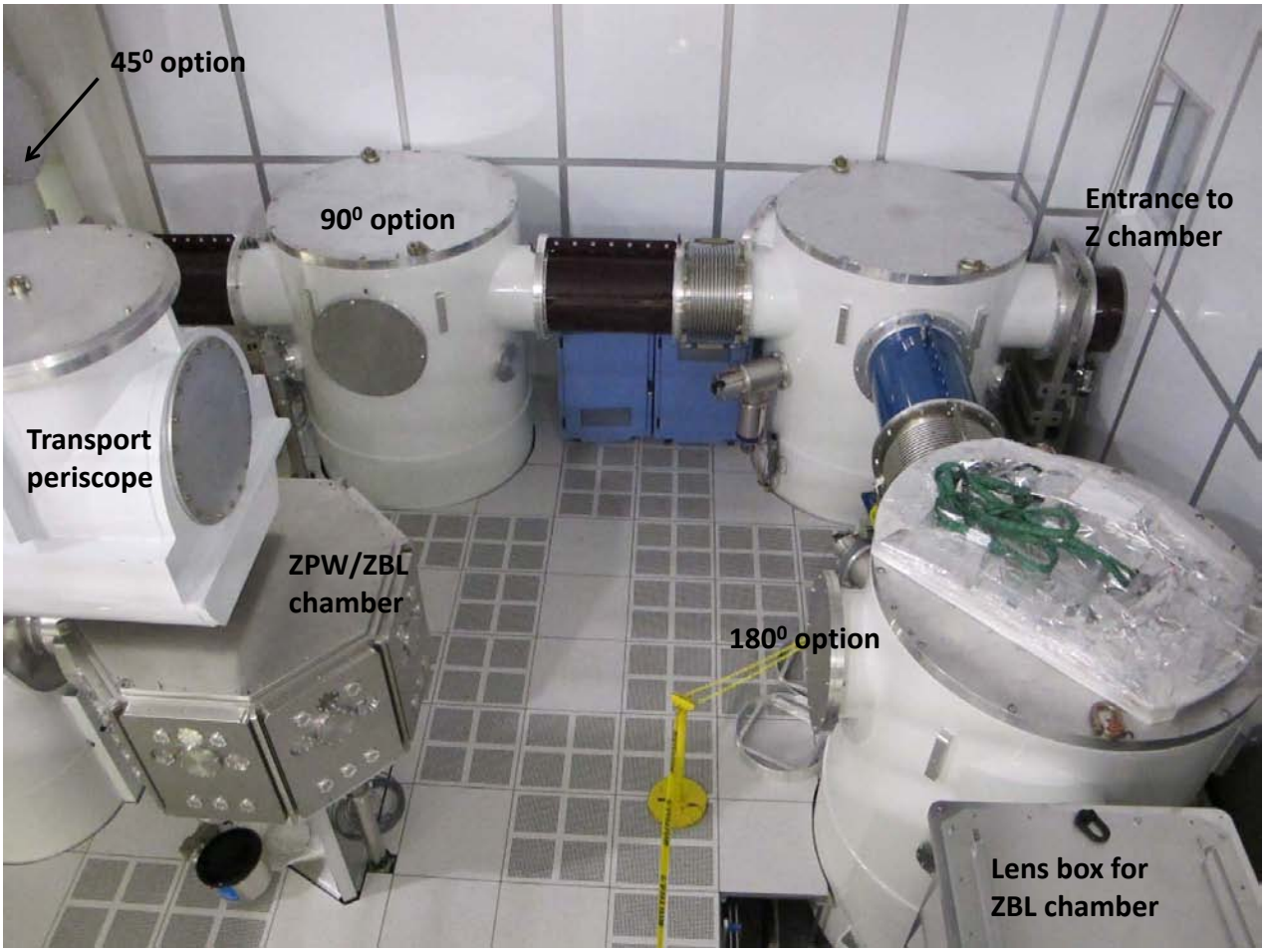

Figure 13. Target Bay as of March 2011. One can see the color coded beam lines as well as the ZPW/ZBL target chamber.

- A target area for testing of new capabilities and advanced experiments is being built. This area will add three additional chambers to our facility and will allow for beam combination of ZPW and Z-Beamlet. The additional chambers will augment existing capabilities and increase experimental output.

All these enabling technologies will pave the way for short/long pulse, multi-frame, multi-color x-ray backlighting at the Z-Accelerator in years to come.

ACKNOWLEDGMENTS

Sandia is a multi-program laboratory operated by Sandia Corporation, a Lockheed Martin Company, for the United States Department of Energy's National Nuclear Security Administration under contract DE-AC04-94AL85000.

REFERENCES

[1] Rambo, P., Smith, I., Porter, J., Hurst, M., Speas, C., Adams, R., Garcia, A., Dawson, E., Thurston, B., Wakefield, C., Kellogg, J., Slattery, M., Ives, H., Broyles, R., Caird, J., Erlandson, A., Murray, J., Behrendt, W., Neilsen, N., and Narduzzi, J., "Z-Beamlet: A multikilojoule, terawatt-class laser system," *Applied Optics* **44**(12), 2421–2430 (2005).

[2] Matzen, M. K., Sweeney, M. A., Adams, R. G., Asay, J. R., Bailey, J. E., Bennett, G. R., Bliss, D. E., Bloomquist, D. D., Brunner, T. A., Campbell, R. B., Chandler, G. A., Coverdale, C. A., Cuneo, M. E., Davis, J. P., Deeney, C., Desjarlais, M. P., Donovan, G. L., Garasi, C. J., Haill, T. A., Hall, C. A., Hanson, D. L., Hurst, M. J., Jones, B., Knudson, M. D., Leeper, R. J., Lemke, R. W., Mazarakis, M. G., McDaniel, D. H., Mehlhorn, T. A., Nash, T. J., Olson, C. L., Porter, J. L., Rambo, P. K., Rosenthal, S. E., Rochau, G. A., Ruggles, L. E., Ruiz, C. L., Sanford, T. W. L., Seamen, J. F., Sinars, D. B., Slutz, S. A., Smith, I. C., Struve, K. W., Stygar, W. A., Vesey, R. A., Weinbrecht, E. A., Wenger, D. F., and Yu, E. P., "Pulsed-power-driven high energy density physics and inertial confinement fusion research," *Physics of Plasmas* **12**(5), 055503 (2005).

[3] Schwarz, J., Rambo, P., Geissel, M., Edens, A., Smith, I., Brambrink, E., Kimmel, M., and Atherton, B., "Activation of the Z-Petawatt laser at Sandia National Laboratories," *Journal of Physics: Conference Series* **112**, 032020–4 (2008).

[4] Kimmel, M., Rambo, P., Broyles, R., Geissel, M., Schwarz, J., Bellum, J., and Atherton, B., "Optical damage testing at the Z-backlighter facility at Sandia National Laboratories," **7504**, 75041G, SPIE. Laser-Induced Damage in Optical Materials: 2009 1.

[5] "Continuum at www.continuumlasers.com,"

[6] "SNLO was created by Arlee Smith and can be obtained for free at www.as-photonics.com,"

[7] Boyd, R., Britten, J., Decker, D., Shore, B., Stuart, B., Perry, M., and Li, L., "High-efficiency metallic diffraction gratings for laser applications.," *Applied Optics* **34**(10), 1697–706 (1995).

[8] Britten, J., Perry, M., Shore, B., and Boyd, R., "Universal grating design for pulse stretching and compression in the 800-1100 nm range.," *Optics Letters* **21**(7), 540–2 (1996).

[9] "Plymouth Grating Laboratory: www.plymouthgrating.com,"

[10] Britten, J. A., Perry, M. D., Shore, B. W., Boyd, R. D., Loomis, G. E., and Chow, R., "High-efficiency, dielectric multilayer gratings optimized for manufacturability and laser damage threshold," *Laser-Induced Damage in Optical Materials: 1995* **2714**, 511–520 768 (1996). Proceedings of the Society of Photo-Optical Instrumentation Engineers (SPIE).

[11] Chen, C. G., Konkola, P. T., Heilmann, R. K., Joo, C., and Schattenburg, M. L., "Nanometer-accurate grating fabrication with scanning beam interference lithography," *Nano- and Microtechnology: Materials, Processes, Packaging, and Systems* **4936**, 126–134 476 (2002). Proceedings of the Society of Photo-Optical Instrumentation Engineers (SPIE).

[12] Bellum, J., Kletecka, D., Rambo, P., Smith, I., Kimmel, M., Schwarz, J., Geissel, M., Copeland, G., Atherton, B., Smith, D., Smith, C., and Khripin, C., "Meeting thin film design and production challenges for laser damage resistant optical coatings at the Sandia Large Optics Coating Operation," **7504**, 75040C, SPIE. Laser-Induced Damage in Optical Materials: 2009.

[13] "Spica Technologies Inc. at www.spicatech.com,"

[14] Bennett, G., Landen, O., Adams, R., Porter, J., Ruggles, L., Simpson, W., and Wakefield, C., "X-ray imaging techniques on Z using the Z-Beamlet laser.," *Review of Scientific Instruments 13th Topical Conference on High-Temperature Plasma diagnostics 13th Topical Conference on High-Temperature Plasma Diagnostics, 18-22 June 2000, Tucson, AZ, USA* **72**(1), 657–2 (2001).

[15] Sinars, D. B., Bennett, G. R., Wenger, D. F., Cuneo, M. E., and Porter, J. L., "Evaluation of bent-crystal x-ray backlighting and microscopy techniques for the Sandia Z-machine," *Applied Optics* **42**(19), 4059–4071 (2003).

[16] Sinars, D. B., Cuneo, M. E., Bennett, G. R., Wenger, D. F., Ruggles, L. E., Vargas, M. F., Porter, J. L., Adams, R. G., Johnson, D. W., Keller, K. L., Rambo, P. K., Rovang, D. C., Seamen, H., Simpson, W. W., Smith, I. C., and Speas, S. C., "Monochromatic x-ray backlighting of wire-array Z-pinch plasmas using spherically bent quartz crystals," *REVIEW OF SCIENTIFIC INSTRUMENTS* **74**(3), 2202–2205 (2003).

[17] Caird, J. A., Erlandson, A. C., Molander, W. A., Murray, J. E., Robertson, G. K., Smith, I. C., Sinars, D. B., and Porter, J. L., "Z-Beamlet (ZBL) multi-frame back-lighter (MFB) system for ICF/plasma diagnostics," *Journal De Physique Iv* **133**, 943–949 (2006).

[18] Sinars, D. B., Peterson, J., Slutz, S. A., Herrmann, M. C., Yu, E. P., Cuneo, M. E., Smith, I. C., Bennett, G. R., Atherton, B., Porter, J. L., and Wenger, D. F., "Observation of instability growth in a copper Z-pinch target using 2-color monochromatic x-ray backlighting," *IEEE Transactions on Plasma Science* (Images in Plasma Science), to be published (2011).

[19] Park, H. S., Chambers, D. M., Chung, H. K., Clarke, R. J., Eagleton, R., Giraldez, E., Goldsack, T., Heathcote, R., Izumi, N., Key, M. H., King, J. A., Koch, J. A., Landen, O. L., Nikroo, A., Patel, P. K., Price, D. F., Remington, B. A., Robey, H. F., Snavely, R. A., Steinman, D. A., Stephens, R. B., Stoeckl, C., Storm, M., Tabak, M., Theobald, W., Town, R. P. J., Wickersham, J. E., and Zhang, B. B., "High-energy k alpha radiography using high-intensity, short-pulse lasers," *Physics of Plasmas* **13**(5), 56309–1 (2006).

[20] Welch, D. R., Rose, D. V., Cuneo, M. E., Campbell, R. B., and Mehlhorn, T. A., "Integrated simulation of the generation and transport of proton beams from laser-target interaction," *Physics of Plasmas* **13**(6), 063105 (2006 LSP is a software product developed by ATK Mission Research, Albuquerque, NM 87110).

[21] Schwarz, J., Rambo, P., Kimmel, M., Geissel, M., Robertson, G., Ramsey, M., Headley, D., and Atherton, B., "Debris mitigation techniques for petawatt-class lasers in high debris environments," *Physical Review Special Topics-Accelerators and Beams* **13**(4), 041001 (2010).